Acta Neuropathol (2012) 124:273–283
DOI 10.1007/s00401-012-0982-8

ORIGINAL PAPER

Next generation sequencing for molecular diagnosis of neuromuscular diseases

Nasim Vasli · Johann Böhm · Stéphanie Le Gras · Jean Muller · Cécile Pizot · Bernard Jost · Andoni Echaniz-Laguna · Vincent Laugel · Christine Tranchant · Rafaelle Bernard · Frédéric Plewniak · Serge Vicaire · Nicolas Levy · Jamel Chelly · Jean-Louis Mandel · Valérie Biancalana · Jocelyn Laporte

Received: 4 March 2012 / Revised: 5 April 2012 / Accepted: 5 April 2012 / Published online: 18 April 2012

Abstract Inherited neuromuscular disorders (NMD) are chronic genetic diseases posing a significant burden on patients and the health care system. Despite tremendous research and clinical efforts, the molecular causes remain unknown for nearly half of the patients, due to genetic heterogeneity and conventional molecular diagnosis based on a gene-by-gene approach. We aimed to test next generation sequencing (NGS) as an efficient and cost-effective strategy to accelerate patient diagnosis. We designed a capture library to target the coding and splice site sequences of all known NMD genes and used NGS and DNA multiplexing to retrieve the pathogenic mutations in patients with heterogeneous NMD with or without known mutations. We retrieved all known mutations, including point mutations and small indels, intronic and exonic mutations, and a large deletion in a patient with Duchenne muscular dystrophy, validating the sensitivity and reproducibility of this strategy on a heterogeneous subset of NMD with different genetic inheritance. Most pathogenic mutations were ranked on top in our blind bioinformatic

J. Böhm and S. Le Gras contributed equally to this article.

Electronic supplementary material The online version of this article (doi:10.1007/s00401-012-0982-8) contains supplementary material, which is available to authorized users.

N. Vasli · J. Böhm · S. Le Gras · J. Muller · C. Pizot · B. Jost · F. Plewniak · S. Vicaire · J.-L. Mandel · V. Biancalana · J. Laporte (✉)
IGBMC (Institut de Génétique et de Biologie Moléculaire et Cellulaire), 1, rue Laurent Fries, BP10142, 67404 Illkirch, France
e-mail: jocelyn@igbmc.fr

N. Vasli · J. Böhm · S. Le Gras · J. Muller · C. Pizot · B. Jost · F. Plewniak · S. Vicaire · J.-L. Mandel · V. Biancalana · J. Laporte
U964, Inserm, Illkirch, France

N. Vasli · J. Böhm · S. Le Gras · J. Muller · C. Pizot · B. Jost · F. Plewniak · S. Vicaire · J.-L. Mandel · V. Biancalana · J. Laporte
UMR7104, CNRS, Illkirch, France

N. Vasli · J. Böhm · S. Le Gras · J. Muller · C. Pizot · B. Jost · F. Plewniak · S. Vicaire · J.-L. Mandel · V. Biancalana · J. Laporte
Université de Strasbourg, Illkirch, France

N. Vasli · J. Böhm · J. Muller · C. Pizot · J.-L. Mandel · V. Biancalana · J. Laporte
Chaire de génétique humaine, Collège de France, Illkirch, France

J. Muller · J.-L. Mandel · V. Biancalana
Laboratoire Diagnostic Génétique, Faculté de Médecine, CHRU, Strasbourg, France

A. Echaniz-Laguna · C. Tranchant
Département de Neurologie, Hôpital Civil de Strasbourg, Strasbourg, France

V. Laugel
Service de Pédiatrie, Centre Hospitalier Universitaire (CHU), Strasbourg, France

R. Bernard · N. Levy
Faculté de Médecine de Marseille, Inserm UMRS 910 Génétique Médicale et Génomique Fonctionnelle, Université de la Méditerranée, Marseille, France

J. Chelly
Institut Cochin, INSERM Unité 1016, CNR UMR 1408, Université Paris Descartes, Sorbonne Paris Cité, Paris, France

pipeline. Following the same strategy, we characterized probable *TTN*, *RYR1* and *COL6A3* mutations in several patients without previous molecular diagnosis. The cost was less than conventional testing for a single large gene. With appropriate adaptations, this strategy could be implemented into a routine genetic diagnosis set-up as a first screening approach to detect most kind of mutations, potentially before the need of more invasive and specific clinical investigations. An earlier genetic diagnosis should provide improved disease management and higher quality genetic counseling, and ease access to therapy or inclusion into therapeutic trials.

Keywords Neuromuscular disorder · Sequencing · Molecular diagnosis · DNA barcoding · Myopathy · Neuropathy

Introduction

Inherited neuromuscular disorders (NMD) form a group of genetic diseases which result in chronic long term disability posing a significant burden to the patients, their families and public health care. NMD are often severe and include more than 200 monogenic disorders with a total incidence exceeding 1 in 3,000 [3]. Despite tremendous research and clinical efforts, the molecular causes of NMD are still unknown for approximately half of patients. The precise diagnosis of NMD requires an extensive clinical evaluation in conjunction with targeted complementary tests. To date, routine genetic diagnosis is mainly done on a gene-by-gene basis, starting from the most pertinent one. Diagnostic challenges in this group of diseases include genetic heterogeneity in most of the disorders and lack of segregation data in sporadic cases to orient the screening. As an example, hereditary sensorimotor neuropathies (HSMN) are due to mutations in nearly 50 genes, while congenital myopathies implicate at least 14 different genes [21, 22]. Also, large genes, such as Titin (*TTN*) with 363 exons, are not entirely sequenced even if previously linked to NMD [1]. As a consequence, clinical tests are multiplied, DNA is sent to different laboratories and patients are submitted to thorough examination that includes sometimes invasive investigations. Often genetic diagnosis is delayed, exposing the patient to unnecessary investigations and treatments, precluding the full benefit of a targeted approach to treatment, and increasing recurrence risk in the families.

Current molecular diagnostic approaches are time-consuming and expensive. Recently, massively parallel sequencing using next generation sequencing (NGS) technologies has emerged as a successful approach to interrogate multiple genes simultaneously and is currently mainly used to identify novel disease genes in a research setting [10, 18–20, 31]. A fewer studies reported the use of whole genome (WGS) or whole exome (WES) sequencing for genetic diagnosis of a given monogenic disease. Concerning NMD, Lupski et al. [14] and Montenegro et al. [16], respectively, used WGS and WES in patients with hereditary sensorimotor neuropathies (HSMN) on a research setting. In both cases, they analyzed a single family and focused their variants ranking only on known HSMN genes. Targeted resequencing of known disease genes appears more relevant for routine diagnosis and until now was tested on a few specific disease genes like 5 ataxia genes or 21 breast cancer genes or a single large gene like *DMD* in very homogeneous patient cohorts, or for carrier testing [6, 13, 30].

As no previous large scale sequencing study targeting several NMD genes was reported, our aim here is to pilot an efficient screening strategy in an attempt to improve the clinical and molecular investigations of neuromuscular diseases from a very heterogeneous panel of patients. We used targeted enrichment of 267 known NMD genes followed by NGS in patients affected by different neuromuscular diseases with or without known mutations. DNA multiplexing and blind variant ranking retrieved successfully different mutation types for diseases with different segregations.

Patients and methods

Patients

Two groups of patients with various neuromuscular diseases were selected: eight patients with pathogenic mutations previously identified by conventional Sanger sequencing of candidate genes (patients A to H), and eight random patients without known mutations and different clinical diagnosis encompassing myopathies and neuropathies (patients I to P). Clinical and segregation data are listed in the online resource data. DNA was extracted from venous blood by three different methods: two manual methods, FlexiGene DNA kit (Qiagen GmbH, Hilden, Germany) and Bacc Nucleon 3 (Amersham-Bioscience), and one automated method, the QIA symphony DNA midi kit (Qiagen GmbH, Hilden, Germany). Informed consent was obtained from all individuals, and the study was approved by the comité de protection des personnes (DC-2012-1497).

Targeted massively parallel sequencing

All the 267 NMD genes, known to be implicated in 16 different disease classes (online resource Table 1; http://www.musclegenetable.org/[8]) were targeted for enrichment. Capture design was done using the Agilent eArray (http://earray.chem.agilent.com/earray/). In this pilot study, we

included the 267 genes because genetic heterogeneity exists in all disease classes and several genes are implicated in different classes (e.g. *LMNA* or *DNM2*). Oligonucleotides covered all coding exons and all intron–exon boundaries including at least 50 intronic nucleotides. 5′ and 3′ UTRs and deep intronic sequences were not targeted to avoid increasing the sequence target size that would have strongly decreased the mean sequence coverage. After masking the repetitive elements, the 4,604 targeted exons represented 1.6 Mb (online resource Table 2). A minimum of 3 µg of genomic DNA was sheared to obtain a mean fragment size of 250 nt using Covaris E210 (KBioscience, Herts, UK) followed by automatic library preparation with the SPRI-TE Nucleic Acid Extractor (Beckman Coulter Inc, Brea, CA) using the SPRIworks fragment library cartridge (Beckman Coulter Inc, Brea, CA) and Illumina adapters. Targeted regions were captured using the Agilent SureSelect custom target enrichment kit (Agilent Technologies, Santa Clara, CA) following Agilent protocols. Enriched DNA fragments were barcoded with the Illumina multiplexing sample preparation kit (Illumina, San Diego, CA), pooled by 4, and sequenced on an Illumina Genome Analyzer IIx to generate 72nt paired-end reads for 4 DNAs per channel, following the manufacturer's protocols.

Bioinformatic analysis

The authors implicated in the sequencing and bioinformatic analysis had no information on the patient data, except for the disease class and potential segregation. The bioinformatic analysis pipeline is depicted in Fig. 1. Image analysis and base calling were performed using the Illumina Pipeline RTA (Real-Time Analysis) version 1.9. DNA sequences were aligned to the reference genome GRCh37/hg19 using BWA [11]. Insertions or deletions of up to 50nt were allowed for the alignment to the genome. Reads that mapped to several positions in the genome and reads sharing the same start position and strand were filtered out using Picard (http://picard.sourceforge.net/) and Samtools [12]. From an average of 14 million mapped reads, about 4 million were uniquely mapped in targeted regions. Valid variants had to be seen in both directions with at least 3× coverage and their calling was done using Samtools; minimum mapping quality was 25, consensus quality was 20 and minimum SNV (single nucleotide variation)/indel quality was 20. Variants were defined as homozygous, if present in more than 80 % of the reads. For SNV/indel annotation SVA (v1.02) [4] (http://www.svaproject.org/), Ensembl60 and dbSNP134 were used, and validated non-pathogenic variants present in dbSNP and 1000Genomes databases were removed.

Variants filtering and ranking were done using the VaRank program. Briefly, for each variant, VaRank used

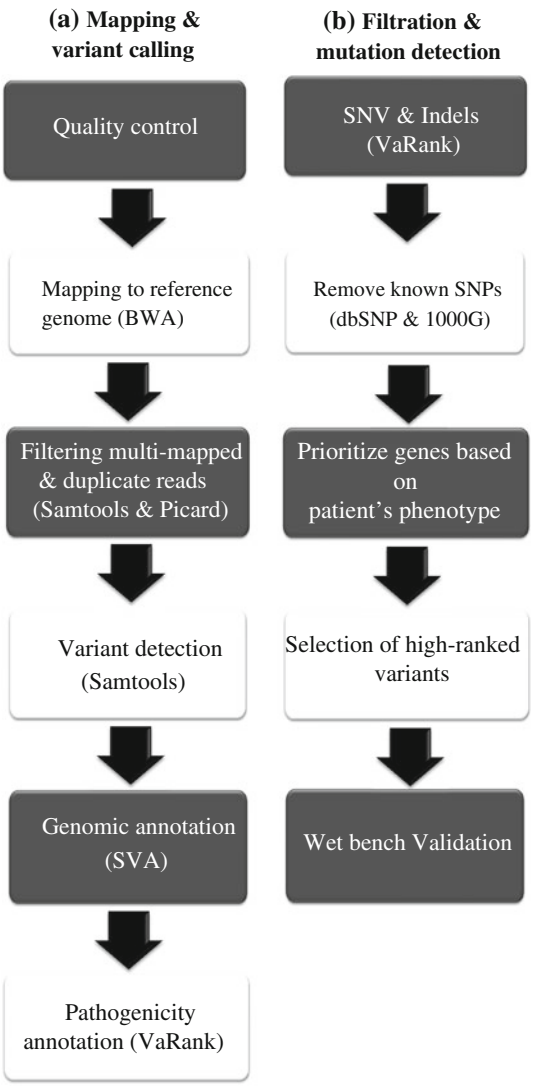

Fig. 1 Bioinformatic filtering and ranking

the Alamut software (Interactive Biosoftware, Rouen, France) to collect genomic annotations and different scores such as the coding status, the nucleotide and amino acid conservation scores and the effect of each change on the protein and splice site, and then compiles them to rank SNVs and indels starting from the most probable pathogenic. The SNVs/indels are characterized using several genomic or functional annotations that VaRank summarizes into a score to produce a list of ranked variants (manuscript in preparation). The probable mutations are ranked starting from the most likely to be pathogenic according to the following list: nonsense, frameshift, essential splice site (affecting the conserved consensus intronic positions), start loss, stop loss, missense, predicted splice site mutation (outside of the consensus sites), in frame indels, and synonymous coding. The scores are modulated according to the genomic conservation based on

the phastcons score [7] and to the SIFT [17] and PolyPhen v2 [23] scores to assess the effect of amino acid change on the protein function. Synonymous coding variants might have an effect on the biosynthesis of the protein [28], and their potential impact on splicing was also scored. Splicing effect is assessed using three different softwares: Human Splicing Finder [2], MaxEntScan [32] and NNSplice [24]. Scores of compound heterozygous mutations in the same gene were added in case of a recessive segregation of the disease to prioritize the best candidate genes. Clinical significance was extracted from dbSNP134 and some of the known mutations were confirmed using locus-specific mutation data bases (LSDB-http://www.umd.be/). The "Clinical significance" field from dbSNP highlights known mutations with an "rs" identifier. Variants annotated as "probably-pathogenic" or "pathogenic" usually corresponded to reported mutations and were weighted to reach a high VaRank score. Indeed, these variants were not filtered as some healthy people are carriers of mutations. In the next step, genes within the patient disease class(es) were extracted and the mode of inheritance of the disease in the family, if known, was matched to the known type of transmission for every selected candidate genes.

In order to detect large deletions, a coverage-based method was used where the number of reads in a sliding window of 20nt was computed across the genome for each patient and coverage compared to three randomly selected patients.

Mutation validation

Sanger sequencing was performed to confirm sequence variants in the original DNA samples and to assess the segregation in the families included in this study (GATC Biotech).

Results

Sequencing results

Following DNA barcoding and pooling by group of 4, targeted sequencing of the 267 known NMD genes (online resource Table 1) was performed in 8 individuals (A to H) with different neuromuscular disorders and known mutations. After alignment with the human reference genome, mean coverage of the targeted exons was 138× and the percentage of nucleotides with at least 10× coverage was 94 (Table 1, online resource Table 2). Average enrichment for targeted exons was 1,410 fold. More than 97 % of the targeted exons were fully covered, while 168 targeted exons were covered <3× in at least half of the patients (online resource Fig. 1 a and online resource Table 2). Most low-covered exons were similar between patients and coverage decreased with increasing GC content (online resource Fig. 1b). Similar findings were obtained in an independent experiment with six of these DNA samples sequenced individually, validating the multiplexing approach (data not shown). DNAs prepared with different extraction protocols gave similar results, supporting the use of these different protocols on a routine diagnosis basis. Reproducibility between different DNAs treated in the same experiment was such that the coverage was similar for given targeted exons (online resource Table 2 and online resource Fig. 2; narrow distribution of the 95th percentile close to the median). This allowed the detection of the copy number to unambiguously determine the gender of patients as a control for the experiment (Fig. 2a, b), and the mapping of a large deletion (see below).

Variants identification and ranking

Variants were identified based on the bioinformatic analysis encompassing sequence mapping, variant calling and filtering, and variant ranking (Fig. 1). On average, we found 1,162 SNVs and 152 indels of which 341 were not reported as SNP (Table 1). 125 variants affecting the essential splice sites or predicted to change the amino acid sequence were found on average in the 267 NMD genes. For prioritization, these variants were ranked using a novel scoring program (VaRank; see methods), then by extracting the different genes fitting the disease class(es) based on the general clinical phenotype of patients, and lastly based on the segregation if known (Table 2 and online resource Table 3). For patients with phenotypes that matched to several disease classes, all genes fitting the different diseases classes were considered.

Identification and confirmation of mutations

We retrieved all ten different known mutations in the eight analyzed DNAs (Table 2; patients A–H). Sequencing data sustaining the mutations are depicted in (Fig. 3a–d and online resource Fig. 4). In particular, we detected homozygous and heterozygous mutations validating the detection of both alleles, point mutations or small insertion or deletions, intronic and exonic mutations. Compound heterozygous mutations in *SETX* were retrieved in the two patients with ataxia (Fig. 3 and online resource Fig. 3). Importantly, our VaRank scoring program blindly ranked the known mutations and implicated genes first in the list when taking into account the disease class and inheritance for most patients (online resource Table 3). Although the clinical data are important to define the disease class, we did not prioritize genes within each disease class based on more detailed pathological data (e.g. even if patient E had myotubular myopathy, all congenital myopathy genes were ranked), suggesting that this approach may be proposed for

Table 1 Sequencing, coverage and variant statistics

	Samples	A	B	C	D	E	F	G	H	Average
Sequencing	Sequenced nucleotides	1179572688	1143805104	749145888	1057816944	1281453552	921756240	912120912	913302000	1019871666
	Sequence after filtering (in nt)[b]	399768120	392297112	314103240	246193344	355696416	351273528	404841528	210318840	334311516
	Sequence in target regions (in nt)	316579968	321670656	249903072	193743144	271231344	274046688	220871448	169312104	252169803
Coverage	Mean coverage (x)	172	176	137	106	148	150	120	96	138
	Median coverage (x)	165	162	126	105	145	144	113	91	131
	% Base ≥3× coverage	98	97	97	98	98	98	97	97	98
	% Base ≥10× coverage	95	94	92	94	95	94	93	93	94
	Fully covered exons	4,477	4,445	4,396	4,443	4,484	4,445	4,429	4,425	4,443
Variants	SNVs	1,097	1,096	1,015	1,148	1,374	1,315	1,127	1,120	1,162
	Indels	208	148	127	139	168	153	127	146	152
	Total heterozygotes	1,018	920	779	973	1,141	1,095	910	859	962
	Total homozygotes	287	324	363	314	401	373	344	407	352
	SNVs + indels	1,305	1,244	1,142	1,287	1,542	1,468	1,254	1,266	1,314
	SNVs + indels without rs number	374	325	259	294	457	403	335	279	341
	Novel coding non-synonymous[a]	111/0	109/0	93/0	99/0	145/0	155/1	116/0	94/1	115/n.a.[c]
	Novel splice site change[a]	10/0	6/0	4/0	4/1	17/0	6/0	5/1	2/0	7/n.a.[c]
	Novel coding stop (gained/lost)[a]	3/0	4/1	0/0	0/0	0/0	1/0	1/0	1/0	1/n.a. [c]
	Novel coding frameshift[a]	3/1	1/0	1/large deletion	2/1	3/1	1/0	2/0	1/1	2/n.a.[c]

Average enrichment is 1,410 fold

[a] Before/after filtering and ranking

[b] After filtering duplicate reads and multiple genomic mapping

[c] Not applicable

patients prior to extensive histological investigations. Moreover, the patients in our cohort were affected by diverse diseases of different segregation (X-linked, autosomal recessive or dominant; Table 2), validating this approach for a wide range of heterogeneous diseases and mutation types.

The large deletion encompassing exons 18–44 of the *DMD* gene was detected in a patient with Duchenne Muscular Dystrophy by comparing the number of reads in these regions with other sequenced DNA samples (Fig. 2b). The mean coverage for exons 18–44 is 0 for this patient and 177 for other patients (online resource Table 2, *DMD* gene for patient C). Unexpectedly, off-target reads from genomic DNA fragments not targeted for enrichment and located in *DMD* introns allowed to restrict the areas containing the upstream and downstream breakpoints from 27 to 11 Kb and 248 to 72 Kb, respectively (Fig. 2c). To assess the accuracy of deletion breakpoints predicted through off-target reads with the precise deleted positions, we analyzed this *DMD* deletion using the custom-designed oligonucleotides CGH-array previously described by Saillour et al. [27] where oligonucleotide probes cover both intronic and exonic *DMD* regions with an average tiling interval of 50 bases. CGH-array indicated that the 3′ breakpoint maps between 32,187,417 (position of the non-deleted probe) and 32,187,427 (position of the deleted probe), and the 5′ breakpoint maps between 32,538,435 and 32,538,443 (Fig. 2d). NGS data are coherent with CGH-array as the off-target reads closer to the deletion mapped at positions 32,072,428 and 32,547,130. The differences between the precise positions based on CGH-array and breakpoints found by NGS data are 115 kb for the 3′ breakpoint and 9 kb for the 5′ breakpoint. For a better precision of NGS method for mapping intronic breakpoints, targeting for enrichment of intronic sequences could be a possibility, but will increase the total targeted sequence length and thus decrease the overall coverage for a given sequencing depth.

Following a similar strategy, we analyzed 8 DNAs (I to P) from patients with heterogeneous neuromuscular disorders without molecular characterization. These patients were not selected based neither on the amount or quality of clinical data nor on the availability of DNA from other members of the family, to mimic the situation of routine

diagnosis. There were no specific inclusion criteria. We identified probable disease-causing mutations in several patients. Sanger sequencing was used to validate the presence of mutations in the original DNA and also confirmed disease segregation (Fig. 3e–f, Table 2, and online resource Fig. 4). Sequencing, coverage and variant statistics were similar to the previous experiment (online resource Table 4). The identified mutations in *RYR1*, *TTN* and *COL6A3* genes were in agreement with the clinical data (online resource data for patient descriptions). Importantly, while variants ranking can be made without

Fig. 2 Detection of copy number and mapping of a deletion in patient C with DMD. **a**, **b** Gender determination: comparison of sequence reads mapping to the X chromosome between two female DNAs in (**a**) and a female (*black*) and a male (*red*) in (**b**). In **b** a deletion of several exons is detected on the X chromosome for the male (*squared*). **c** Next generation sequencing data showing the detection of a 27 exons deletion in patient C with DMD (*middle panel*) compared to two other DNAs (*top and bottom panels*). Random off-target reads allow a more precise mapping of the deletion breakpoints. Off-target reads varied between two different experiments. **d** CGH-array results showing the 5′ and 3′ breakpoints map between 32,538,435 and 32,538,443 and between 32,187,417 and 32,187,427, respectively

Table 2 Mutations identified in patients with known mutations and probable mutations in patients without previous molecular characterization

Patient	Gender	Disease (segregation)	Disease class	Gene	Mutation nucleotide (protein)	Haplotype
A	F	Carrier for myotubular myopathy (XL)	Congenital myopathies	*MTM1*	Exon4: c.141–144delAAAG (p.Glu48LeufsX24)	Heterozygous
B	M	Centronuclear myopathy (AR)	Congenital myopathies	*BIN1*	Exon20: c.1717 C > T (p.Gln573X)	Homozygous
C	M	Duchenne muscular dystrophy (XL)	Muscular dystrophies	*DMD*	Deletion ex18-44	Hemizygous
D	F	Ataxia ocular apraxia (AR)	Hereditary ataxias	*SETX*	Exon10: c.3213–3214insT (p.Gln1072SerfsX3); Int10: c.5275-1 G > A	Compound heterozygous
E	M	Myotubular myopathy (XL)	Congenital myopathies	*MTM1*	Exon4: c.156–157insA (p.Cys53MetfsX8)	Hemizygous
F	F	Centronuclear myopathy (AD)	Congenital myopathies	*DNM2*	Exon14: c.1565G>A (p.Arg522His)	Heterozygous
G	M	Myotubular myopathy (XL)	Congenital myopathies	*MTM1*	Int11: c.1261–10A>G	Hemizygous
H	F	Ataxia ocular apraxia (AR)	Hereditary ataxias	*SETX*	Exon10: c.2967-2971delGAAAG (p.Arg989SerfsX5); Exon8: c.994C>T (p.Arg332Trp)	Compound heterozygous
I	M	HMSN, demyelinating CMT neuropathy (AR)[a]	n.a.[a]	None		
J	M	Myopathy with cytoplasmic aggregates	All myopathies	*TTN*[c]	Exon292: c.68576C>T (p.Pro22859Leu)	Heterozygous
K	F	Bethlem dystrophy or myofibrillar myopathy (AD)	Muscular dystrophies, other myopathies	*COL6A3*[c]	Exon27: c.6812G>A (p.Arg2271Lys)	Heterozygous
L	M	Hereditary spastic paraplegia (sporadic)	Hereditary paraplegias	None		
M	M	Vacuolar myopathy (sporadic)	Congenital myopathies, distal myopathies, other myopathies	None		
N	M	HMSN, axonal CMT (AR)	Hereditary neuropathies	None (LMNA)	Exon11: c.1928C>A (p.Thr643Asn); c.1930C>T (p.Arg644Cys)[b]	Compound heterozygous
O	F	Muscular dystrophy (AR)	Muscular dystrophies	*TTN*[c]	Exon18: c.3100G>A (p.Val1034Met); Exon240: c.49243G>A (p.Ala16415Thr)	Compound heterozygous
P	M	Muscular dystrophy and arthrogryposis (AR)	Muscular dystrophies, congenital myopathies, other NMD diseases	*RYR1*[c]	Exon55: c.8554C>T (p.Arg2852X); Exon81: c.11557G>A (p.Glu3853Lys)	Compound heterozygous

[a] *HMSN* hereditary motor and sensory neuropathy, *CMT* Charcot–Marie–Tooth; patient I was later re-diagnosed as having a mitochondrial disease for which genes were not targeted

[b] Previously reported as pathogenic; probable monoallelic compound heterozygous

[c] Confirmed by segregation analysis

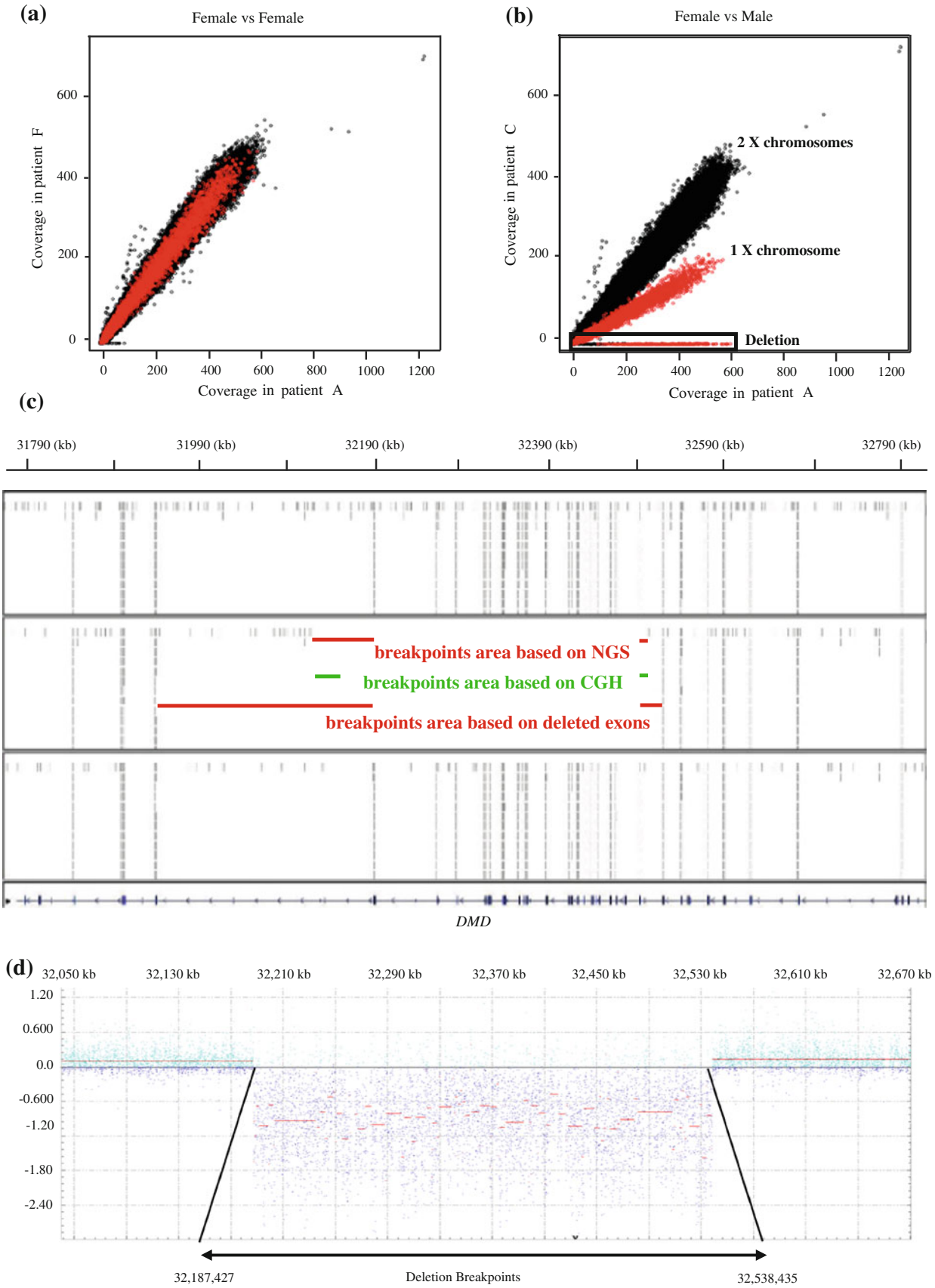
(a)
Female vs Female
Coverage in patient F
Coverage in patient A
(b)
Female vs Male
Coverage in patient C
2 X chromosomes
1 X chromosome
Deletion
Coverage in patient A
(c)
31790 (kb)
31990 (kb)
32190 (kb)
32390 (kb)
32590 (kb)
32790 (kb)
breakpoints area based on NGS
breakpoints area based on CGH
breakpoints area based on deleted exons
DMD
(d)
32,050 kb
32,130 kb
32,210 kb
32,290 kb
32,370 kb
32,450 kb
32,530 kb
32,610 kb
32,670 kb
1.20
0.600
0.0
-0.600
-1.20
-1.80
-2.40
32,187,427
Deletion Breakpoints
32,538,435

(a) *SETX* **: c.994C>T, p.Arg332Trp**
heterozygous exonic point mutation
patient H

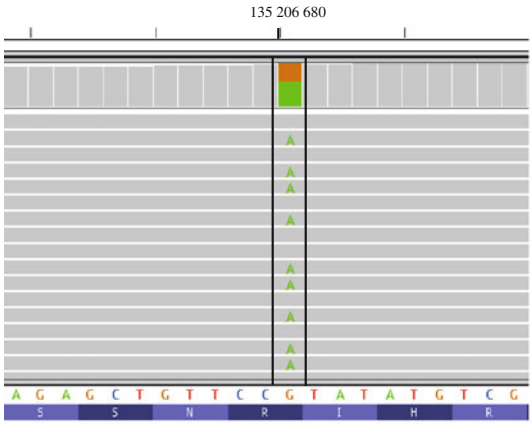

SETX (NM-015046.5)

(b) *SETX* **: c.2967_2971del, p.Arg989SerfsX5**
heterozygous deletion
patient H

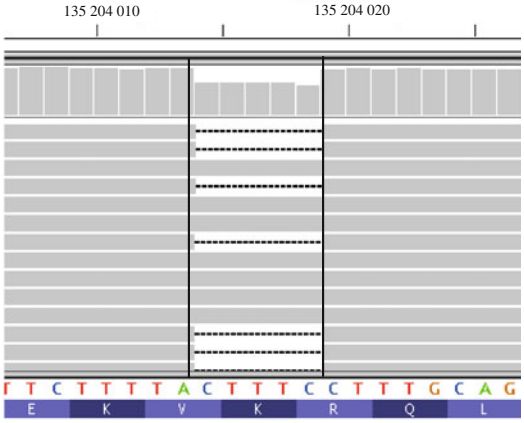

SETX (NM-015046.5)

(c) *BIN1* **: c.1717C>T, p.Gln573X**
homozygous exonic point mutation
patient B

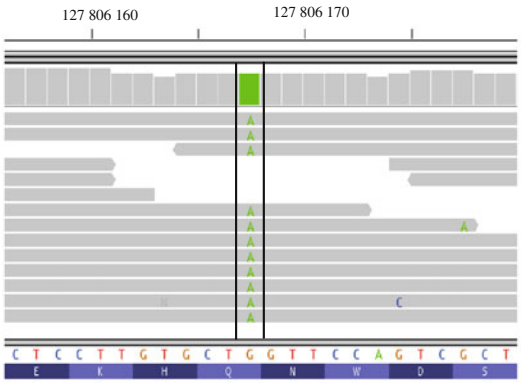

BIN1 (NM_139343.1)

(d) *MTM1* **: In11 c.1261-10A>G**
hemizygous intronic mutation
patient G

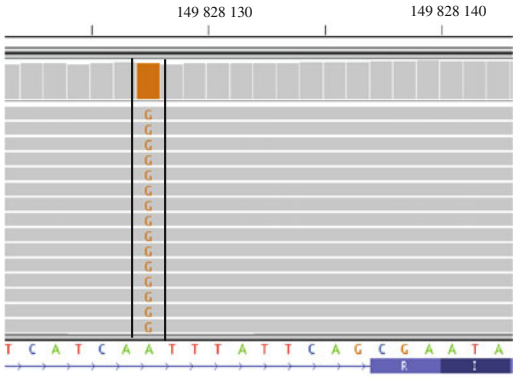

MTM1 (NM_000252.2)

(e) *RYR1* **: c.8554C>T, p.Arg2852X**
heterozygous exonic point mutation
patient P

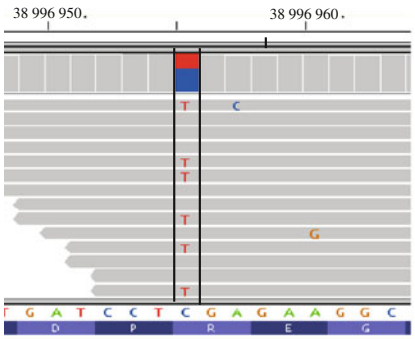

RYR1 (NM_000540.2)

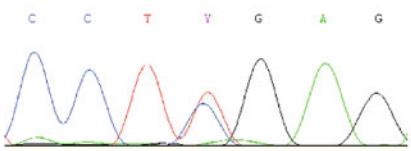

(f) *RYR1* **: c.11557G>A, p.Glu3853Lys**
heterozygous exonic point mutation
patient P

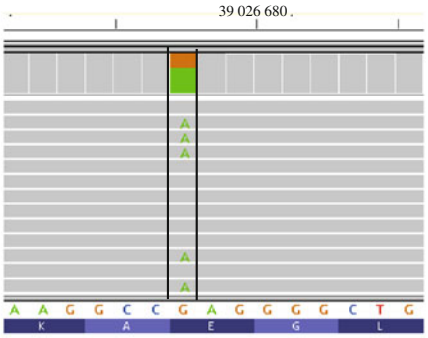

RYR1 (NM_000540.2)

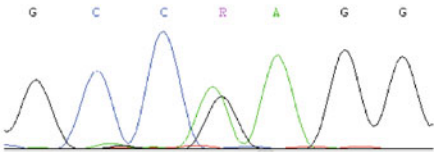

◀**Fig. 3** Detection of different types of mutations from patients with previously known and unknown molecular diagnosis. Compound heterozygous exonic point mutation (**a**) and heterozygous indel mutation (**b**) in the *SETX* gene in patient H with ataxia. **c** Homozygous exonic point mutation in the *BIN1* gene in patient B with centronuclear myopathy. **d** Intronic mutation in the *MTM1* gene in patient G with myotubular myopathy. **e**, **f** Novel compound heterozygous mutations detected in patient P with muscular dystrophy and arthrogryposis in the *RYR1* gene by next generation sequencing and confirmed by Sanger sequencing. Displayed with the integrative genomics viewer IGV [25]. The normal nucleotide and protein sequences are depicted at the *bottom*

detailed clinical and histological data to suggest probable mutated genes, such data are very valuable to validate the molecular findings. For example, we identified compound heterozygous mutations (including a nonsense mutation) in the ryanodine receptor (*RYR1)* in patient P presenting with muscular dystrophy and arthrogryposis (Fig. 3e–f). Indeed *RYR1* mutations have previously been linked to several congenital myopathies, [29] and also to severe neonatal arthrogryposis [26]. The mutations were found in his affected twin brother and each parent was found to be heterozygous for one mutation. We also identified probable mutations in the large *TTN* gene in patients J and O with myopathy with cytoplasmic aggregates and limb girdle muscular dystrophy, respectively, widening the clinical and molecular spectra for this gene that is not routinely sequenced on a diagnosis setting due to its large size.

We did not have false negative in the eight patients with known mutations as we retrieved all mutations. We checked the rate of false positive, i.e. variant not present in the starting DNA, in patients with unknown mutations where we found the probable disease-causing mutations. We found that the probability of being false positive due to sequencing or mapping errors is high when the percentage of reads showing the change is less than 25 or when the number of reads showing the change is less than 8. Even with these cut-offs, 16.5 % of false positive variants were found out of 40 variants tested, calling for validation of the mutations by Sanger sequencing.

Discussion

In this study, we performed targeted sequencing of the coding sequences and all intron–exon boundaries including at least 50 intronic nucleotides of the known NMD genes through massively parallel sequencing in a cohort of patients with heterogeneous neuromuscular diseases. We were able to retrieve all the known mutations in previously characterized patients and we identified several novel pathogenic mutations in patients lacking molecular diagnosis.

We demonstrate that this strategy can detect several types of mutations including intronic and exonic changes as well as small indel and a large deletion. All mutations were detected from the massively parallel sequencing and analysis of a single proband, unlike previous studies where comparative sequencing of several individual exomes was used to retrieve the causative mutations in a family with HSMN [16]. A main challenge in NGS data analysis is the identification of the pathogenic change among the large list of variants. Our blind analysis based on variant ranking and disease class allowed the identification of all known mutations. However, detailed clinical, histological and molecular data were necessary for the confirmation steps, i.e., matching the genetic data with the phenotype.

Such targeted parallel sequencing of all candidate genes is especially suitable for diseases with high genetic heterogeneity, as it is the case for NMD, and should ease the identification of allelic diseases, i.e., different diseases caused by mutations of the same gene. In addition, this strategy allows the analysis of large genes, such as *TTN*, that are routinely not fully tested by conventional Sanger sequencing even if known to be implicated in diseases. For example, our identification of a probable *TTN* mutation in a patient with myopathy with cytoplasmic aggregates and respiratory insufficiency widen the clinical spectrum compared to previous studies [5].

We did not find disease-causing mutations among the coding sequences of the NMD genes in four patients with unknown genetic cause. Patient I was first clinically diagnosed with demyelinating polyneuropathy, but clinical and biochemical re-analyses in parallel to NGS suggested he had a mitochondrial disease which implicated genes are not covered by our present design. Patient N showed two missense changes in *LMNA* including the p.Arg644Cys change, previously linked to various laminopathies. Both changes are on the same allele, as they were always found in the same reads/fragments (online resource Fig. 4e), and thus cannot be the sole cause of the axonal neuropathy. We did not have access to parent DNAs to investigate this further. For the other two patients, who were previously excluded for several candidate genes by Sanger sequencing, mutations were also missed by our approach. The disease-causing mutation may be a deep intronic change, repeat expansions or translocation for which detection has not been tested in this study. Concerning specifically repeat expansions, they cannot be mapped back to a reference genome unambiguously due to their repetitive nature. Alternatively, these patients may also be mutated in a gene not linked to NMD at the time of our targeting library design.

WGS or WES would in principle allow re-analysis of variants list once newly discovered genes are identified, while these genes should be added to update the NMD capture library. However, these approaches have several disadvantages for routine molecular diagnosis compared to

the *NMD-seq* strategy described in this study, especially concerning design, coverage, variant analysis and validation, incidental findings, and throughput and price. WES capture library should also be updated to incorporate novel gene and exon predictions, and cannot be customized to increase the enrichment of specific exons difficult to capture or incorporate known intronic mutation hotspots. *NMD-seq* has a higher coverage and leads to a smaller list of variants as it focuses on a subset of genes, whereas the sensitivity and heterozygosity assessment decrease following WGS or WES due to lower coverage [31]. Sequencing more genes at a lower coverage leads to an increased risk of false negative and an increased number of false positive variants that are time-consuming to validate. Indeed, WES at 50× mean coverage results in about 20 % of targeted regions covered less than 10 times, outputs not suited for routine diagnosis. WES or WGS also potentiate incidental finding, i.e. the discovery of an unrelated disease not targeted by the diagnosis measure; this could be an ethical issue. Moreover, WGS or WES have lower throughput and a higher cost, both are important issues for routine diagnosis. We validated DNA multiplexing for four DNAs in one channel to increase throughput and decrease the cost in comparison with conventional Sanger approaches which is about 500–1,000 € per sample for one gene but can increase to 5,000 € or more depending on gene size. Testing several candidates on a gene-by-gene basis may exceed 8,000 € [9]. With recent developments in sequencers and DNA barcoding, we estimate the total cost of *NMD-seq* from a pool of 12 barcoded DNAs to about 500 € per patient for at least 140× coverage, while WES and WGS cost about 1,500 € and 5,000 € for a 50× coverage, respectively. It takes about 2 months to perform the NMD-seq approach for 267 genes (excluding validation of the data by Sanger sequencing), a similar turnaround time to what is proposed by diagnosis laboratories to test a gene with 20 exons under current routine diagnosis.

Major conditions for further use of the *NMD-seq* strategy as a routine approach in genetic diagnostic labs are the reproducibility, detection sensitivity and the study of heterogeneous cohort of patients with sometimes incomplete clinical characterization as it was the case in our study. After validation of other types of mutations not tested in this study, this strategy could be implemented as a first screening approach, potentially before the need of more invasive and time-consuming investigations such as biopsies.

Our strategy does not require the knowledge of detailed clinical data for proposing candidate mutations; however, this knowledge is necessary for the final validation of the diagnosis that can only be performed matching both clinical and genetic data. NGS will not replace clinical investigations but rather direct clinicians towards the most adequate investigations, while excluding unnecessary costly and time-consuming tests. As a general rule for all NGS approaches, the targeted regions are not homogeneously covered. This point could most probably be enhanced by increasing the amount of oligonucleotides targeting regions more difficult to enrich. For an exclusion diagnosis, conventional Sanger sequencing of specific exons might be necessary if the best candidate genes for a specific disorder are not well covered by NGS. In any case, mutations found by NGS must be validated by Sanger sequencing to rule out sequence errors introduced during the NGS protocol, to provide a second independent confirmation and a basis for a simplified test for further counseling within the family. Importantly, variant ranking and confirmation depend on clinical data and knowledge on NMD, and are thus probably not directly applicable for direct-to-consumer testing.

A faster molecular diagnosis of NMD will have major impacts on patients as it will improve disease management and genetic counseling, and will allow access to therapy or inclusion into therapeutic trials. As an example, the identification of *RYR1* mutations in patient P is of major medical importance as the treatment of *RYR1* patients with salbutamol has shown significant amelioration of muscle weakness [15]. In conclusion, we provided the first proof-of-principle that next generation sequencing could be apply for molecular diagnosis of neuromuscular disorders.

Acknowledgments We thank Michel Koenig and Mathieu Anheim for DNA samples with known mutations, Ngoc-Hoan Nguyen and Céline Keime for help in the bioinformatics setup and analysis, Claudia Strafella, Nicolas Dondaine, Gabrielle Rudolf, Juliette Nectoux, Céline Leroux, Isabelle Atlan and France Leturcq for technical assistance, and Gisèle Bonne for discussions. This study was supported by the Institut National de la Santé et de la Recherche Médicale (INSERM), the Centre National de la Recherche Scientifique (CNRS), University of Strasbourg (UdS), Collège de France and grants from the Agence Nationale de la Recherche, Muscular Dystrophy Association and Myotubular Trust.

Conflict of interest The authors declare that they have no conflict of interest.

References

1. Bang ML, Centner T, Fornoff F et al (2001) The complete gene sequence of titin, expression of an unusual approximately 700-kDa titin isoform, and its interaction with obscurin identify a novel Z-line to I-band linking system. Circ Res 89:1065–1072
2. Desmet FO, Hamroun D, Lalande M et al (2009) Human Splicing Finder: an online bioinformatics tool to predict splicing signals. Nucleic Acids Res 37:e67

3. Emery AE (1991) Population frequencies of inherited neuromuscular diseases—a world survey. Neuromuscul Disord 1:19–29
4. Ge D, Ruzzo EK, Shianna KV et al (2011) SVA: software for annotating and visualizing sequenced human genomes. Bioinformatics 27:1998–2000
5. Hackman P, Vihola A, Haravuori H et al (2002) Tibial muscular dystrophy is a titinopathy caused by mutations in TTN, the gene encoding the giant skeletal-muscle protein titin. Am J Hum Genet 71:492–500
6. Hoischen A, Gilissen C, Arts P et al (2010) Massively parallel sequencing of ataxia genes after array-based enrichment. Hum Mutat 31:494–499
7. Hubisz MJ, Pollard KS, Siepel A (2011) PHAST and RPHAST: phylogenetic analysis with space/time models. Brief Bioinform 12:41–51
8. Kaplan JC (2010) The 2011 version of the gene table of neuromuscular disorders. Neuromuscul Disord 20:852–873
9. Kingsmore SF, Saunders CJ (2011) Deep sequencing of patient genomes for disease diagnosis: when will it become routine? Sci Transl Med 3:87ps23
10. Levy S, Sutton G, Ng PC et al (2007) The diploid genome sequence of an individual human. PLoS Biol 5:e254
11. Li H, Durbin R (2009) Fast and accurate short read alignment with Burrows-Wheeler transform. Bioinformatics 25:1754–1760
12. Li H, Handsaker B, Wysoker A et al (2009) The Sequence Alignment/Map format and SAMtools. Bioinformatics 25:2078–2079
13. Lim BC, Lee S, Shin JY et al (2011) Genetic diagnosis of Duchenne and Becker muscular dystrophy using next-generation sequencing technology: comprehensive mutational search in a single platform. J Med Genet 48:731–736
14. Lupski JR, Reid JG, Gonzaga-Jauregui C et al (2010) Whole-genome sequencing in a patient with Charcot–Marie–Tooth neuropathy. N Engl J Med 362:1181–1191
15. Messina S, Hartley L, Main M et al (2004) Pilot trial of salbutamol in central core and multi-minicore diseases. Neuropediatrics 35:262–266
16. Montenegro G, Powell E, Huang J et al (2011) Exome sequencing allows for rapid gene identification in a Charcot–Marie–Tooth family. Ann Neurol 69:464–470
17. Ng PC, Henikoff S (2003) SIFT: predicting amino acid changes that affect protein function. Nucleic Acids Res 31:3812–3814
18. Ng SB, Buckingham KJ, Lee C et al (2010) Exome sequencing identifies the cause of a mendelian disorder. Nat Genet 42:30–35
19. Ng SB, Nickerson DA, Bamshad MJ, Shendure J (2010) Massively parallel sequencing and rare disease. Hum Mol Genet 19:R119–R124
20. Ng SB, Turner EH, Robertson PD et al (2009) Targeted capture and massively parallel sequencing of 12 human exomes. Nature 461:272–276
21. North K (2008) What's new in congenital myopathies? Neuromuscul Disord 18:433–442
22. Pareyson D, Marchesi C (2009) Diagnosis, natural history, and management of Charcot–Marie–Tooth disease. Lancet Neurol 8:654–667
23. Ramensky V, Bork P, Sunyaev S (2002) Human non-synonymous SNPs: server and survey. Nucleic Acids Res 30:3894–3900
24. Reese MG, Eeckman FH, Kulp D, Haussler D (1997) Improved splice site detection in Genie. J Comput Biol 4:311–323
25. Robinson JT, Thorvaldsdottir H, Winckler W et al (2011) Integrative genomics viewer. Nat Biotechnol 29:24–26
26. Romero NB, Monnier N, Viollet L et al (2003) Dominant and recessive central core disease associated with RYR1 mutations and fetal akinesia. Brain 126:2341–2349
27. Saillour Y, Cossee M, Leturcq F et al (2008) Detection of exonic copy-number changes using a highly efficient oligonucleotide-based comparative genomic hybridization-array method. Hum Mutat 29:1083–1090
28. Sauna ZE, Kimchi-Sarfaty C (2011) Understanding the contribution of synonymous mutations to human disease. Nat Rev Genet 12:683–691
29. Treves S, Jungbluth H, Muntoni F, Zorzato F (2008) Congenital muscle disorders with cores: the ryanodine receptor calcium channel paradigm. Curr Opin Pharmacol 8:319–326
30. Walsh T, Lee MK, Casadei S et al (2010) Detection of inherited mutations for breast and ovarian cancer using genomic capture and massively parallel sequencing. Proc Natl Acad Sci USA 107:12629–12633
31. Wheeler DA, Srinivasan M, Egholm M et al (2008) The complete genome of an individual by massively parallel DNA sequencing. Nature 452:872–876
32. Yeo G, Burge CB (2004) Maximum entropy modeling of short sequence motifs with applications to RNA splicing signals. J Comput Biol 11:377–394

ActaNeuropathologica

Next generation sequencing for molecular diagnosis of neuromuscular diseases

Nasim Vasli[1,2,3,4,5], Johann Böhm[1,2,3,4,5,$](PhD), Stéphanie Le Gras[1,2,3,4,$], Jean Muller[1,2,3,4,5,6](PhD), Cécile Pizot[1,2,3,4,5], Bernard Jost[1,2,3,4](PhD), Andoni Echaniz-Laguna[7](MD), Vincent Laugel[8](MD), Christine Tranchant[7](MD), Rafaelle Bernard[9](MD), Frédéric Plewniak[1,2,3,4](PhD), Serge Vicaire[1,2,3,4], Nicolas Levy[9](MD, PhD), Jamel Chelly[10](MD, PhD), Jean-Louis Mandel[1,2,3,4,5,6](MD, PhD), Valérie Biancalana[1,2,3,4,5,6](PhD), Jocelyn Laporte[1,2,3,4,5*](PhD).

[1]IGBMC (Institut de Génétique et de Biologie Moléculaire et Cellulaire), Illkirch, France
[2]Inserm, U964, Illkirch, France
[3]CNRS, UMR7104, Illkirch, France
[4]Université de Strasbourg, Illkirch, France
[5]Collège de France, chaire de génétique humaine, Illkirch, France
[6]Laboratoire Diagnostic Génétique, Faculté de Médecine, CHRU, Strasbourg, France
[7]Département de Neurologie, Hôpital Civil de Strasbourg, Strasbourg, France
[8]Service de Pédiatrie, Centre Hospitalier Universitaire (CHU), Strasbourg, France
[9]Faculté de Médecine de Marseille, Université de la Méditerranée, Inserm UMRS 910 Génétique Médicale et Génomique Fonctionnelle, Marseille, France
[10]Institut Cochin, INSERM Unité 1016, CNR UMR 1408, Université Paris Descartes, Sorbonne Paris Cité, Paris, France

[$]Equal contributors
Corresponding author: Dr Jocelyn Laporte

Corresponding author's address: 1, rue Laurent Fries, BP10142, 67404 Illkirch, France.
Corresponding author's phone and fax: Phone: +33 3 88653412- fax: +33 3 88653246

Corresponding author's e-mail address: jocelyn@igbmc.fr

Online Resource data

Enrichment factor

Enrichment factor for the targeted NMD genes, following targeted capture and sequencing, was calculated as the ratio between the total number of sequenced nucleotides related to the total size of the human genome versus the total number of nucleotides on target regions related to the total size of targeted regions.

Clinical and segregation data for patients I-P without previous molecular characterization

Online resource table 3 lists the sequencing data for all patients, the found mutations, the predicted amino acid change effect and the rank of the mutation among all found variants.

Patient I is a 43 year old Algerian man, born from a consanguineous marriage, with an affected sister. He first presented with polyneuropathy since he was 8 years old and he was diagnosed

with recessive demyelinating Charcot-Marie-Tooth disease (CMT4). However, additional clinical investigations showed he was affected by a mitochondrial disease. We did not find any probable mutations in the NMD genes targeted by next generation sequencing, and genes implicated in such diseases were not targeted by the *NMD-seq* capture library.

Patient J is a 56 years-old Portuguese man with isolated respiratory insufficiency since the age of 46. He had no muscle weakness, no muscle wasting, and no dysphagia. CK levels were normal. He had a sister who also presented with isolated respiratory insufficiency. Muscle biopsy demonstrated cytoplasmic body myopathy in both patients. Edstrom et al described patients with similar clinical signs and an autosomal dominant mutation in the kinase domain of TTN [1, 2]. This myopathy was called hereditary myopathy with early respiratory failure (HMERF). In our patient the probable mutation was in the *TTN* gene, thus in accordance with previous findings in these other patients. However, in our patient the mutation is outside of the kinase domain and this may explain the milder presentation of disease in this patient. In our patient, the respiratory insufficiency appeared later in life, widening the clinical severity that can be associated to dominant *TTN* mutation.

Patient K is a 35-year old French woman with a muscular dystrophy resembling either a limb girdle muscular dystrophy or Bethlem/Ullrich syndrome. She developed progressive moderate proximal and also distal muscle weakness since age 20. CK level is normal. Histological data suggested myofibrillar myopathy. Her father is affected with a milder myopathy and her brother also has difficulties to rise from a chair, that may be due to either a congenital hip dislocation or to muscle weakness. This brother has two daughters showing congenital hip dislocation and a very severe neonatal muscle weakness. Assuming they all share the same disease with different clinical expression, none of the candidate genes in patient K were found similarly mutated in all four other affected relatives. However, a probable heterozygous mutation in *COL6A3* is common to patient K, his father and his brother, all sharing similar age of onset and ambulation difficulties. This variant is absent in the unaffected mother. Mutations in the *COL6A3* gene have been previously implicated in other patients with Bethlem/Ullrich syndrome. Based on our sequencing findings, complementary clinical analyses are ongoing to determine whether the different family members suffer from the same disease with strong clinical variability, or whether two diseases segregate in the family.

Patient L is a 5-year old boy affected with familial spastic paraplegia. An affected cousin lives in Turkey and could not be examined. He has walking problems, increased deep tendon reflexes and bilateral Babinski's sign. He also shows some signs of progressive muscle weakness and amyotrophy. Cerebrospinal MRI and CK levels were normal. Muscle biopsy was refused by parents. We couldn't find any variations in genes known to be implicated in spastic paraplegias.

Patient M is a 47-year old French man with vacuolar myopathy. From 30 years old he showed muscle weakness in his legs. He is a sporadic case. We excluded all candidate variants by checking non-affected parents and sister.

Patient N is a 38-year old Algerian man from a consanguineous family. He has axonal hereditary sensorimotor neuropathies (HSMN). One brother and two sisters are affected by the same disease. Following our next generation sequencing and data analysis protocol, two probable heterozygous variations were found in the Lamin A/C gene, including the p.Arg644Cys missense

previously reported as pathogenic in different laminopathies and never found in control populations. However, both variants are on the same allele based on NGS data, as the two changes were always found in the same reads/fragments (Online resource Fig 4e), we favor the implication of a novel gene not targeted by the *NMD-seq* library. Parents DNAs were not available to investigate this further.

Patient O is a 50-year old French woman with limb girdle muscular dystrophy. She has one affected brother. She developed proximal upper and lower limbs weakness since age 35. Symptoms are stable. We found two probable heterozygous mutations in the *TTN* gene by next generation sequencing that were confirmed to be both present in her affected brother by Sanger sequencing. Her mother was carrier of one of the changes in *TTN*, while DNA from the father was not available.

Patient P is a French 13-year old boy with congenital muscular dystrophy and arthrogryposis. He has an affected twin brother. He showed congenital muscle weakness, stiff ankles and knees, feeding problems and respiratory distress at birth. He was never able to walk and later developed severe scoliosis and chronic restrictive respiratory failure. Muscle biopsy showed extensive muscle fiber degeneration and fibrosis, as well as numerous rod inclusions. We found two probable heterozygous mutations in *RYR1* in both twins, including a stop codon, and each parent was heterozygous carrier of one of the variants.

Online resource figures:

Online resource Fig 1: Sequence coverage. a) Number of non-covered exons is depicted for 1 to all 16 patients tested. Non covered exons are exons with coverage less or equal to 2x. Most non-covered exons are similar between samples and GC rich. A full list is found in online resource table 2. b) Coverage depends on GC content as increasing percentage of GC parallels with decreasing nucleotide coverage. Displays patient A data.

a

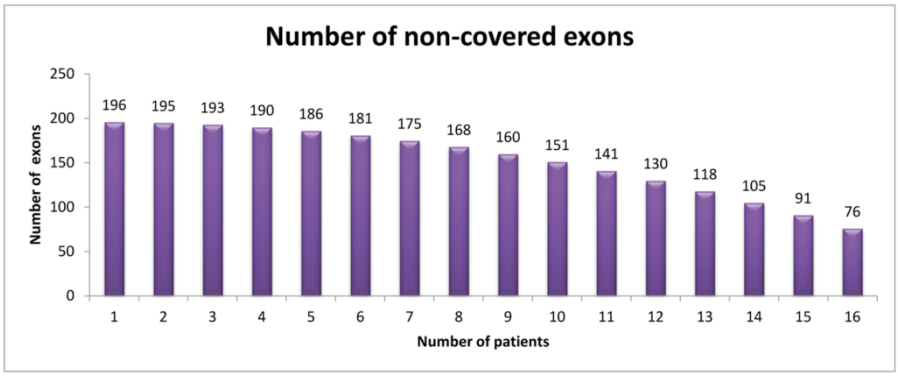

b

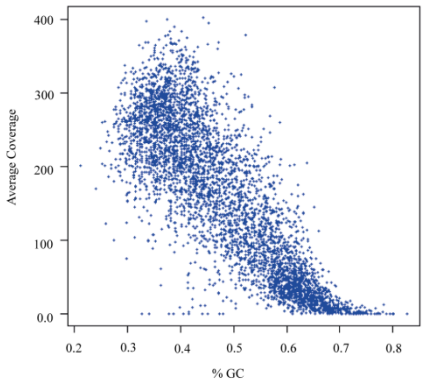

Online resource Fig 2: Coverage in targeted exons
Distribution of average coverage within exons in autosomal chromosomes across all samples tested. Coverage is not homogeneous across all regions; however, coverage is similar across samples at a given position as shown by the narrow distribution. The median has been computed based on the average coverage of all samples.

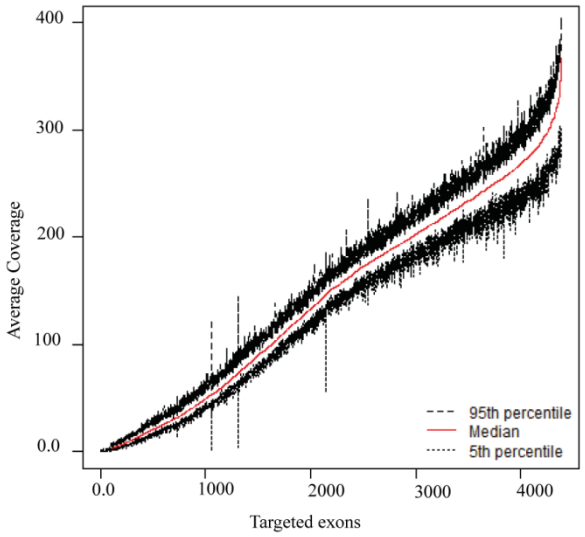

Online resource Fig 3: Detection of different types of mutations. a) Detection of an exonic heterozygous deletion in the *MTM1* gene in a female carrier for X-linked myotubular myopathy (patient A). The mutation in exon 4 is c.141-144delAAAG; p.Glu48fsX24. b) Detection of a hemizygous small insertion in the *MTM1* gene in a patient with X-linked myotubular myopathy (patient E). The mutation in exon 4 is c.156insA; p.Cys53fsX8. c and d) Detection of compound heterozygous mutations in the *SETX* gene in a patient with autosomal recessive ataxia (patient D). The mutations in exons 10 and 11 are c.3213_3214insT; p.Q1072fsX3 and c.5275-1G>A, respectively. e) Detection of a heterozygous exonic point mutation in the *DNM2* gene in a patient with autosomal dominant centronuclear myopathy (patient F). The mutation in exon 14 is c. 1565G>A, p.Arg522His. Figures displayed with the integrative genomics viewer IGV. The normal nucleotide and protein sequences are depicted at the bottom.

a *MTM1*: c.141-144delAAAG, p.Glu48LeufsX24
heterozygous deletion
patient A

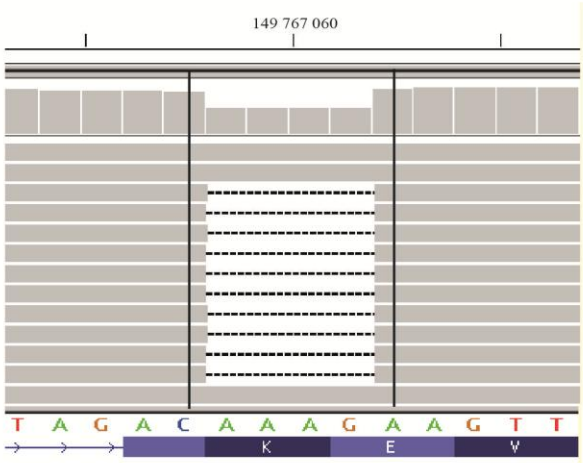

MTM1 (NM_000252.2)

b *MTM1*: c.156-157insA, p.Cys53MetfsX8
hemizygous insertion
patient E

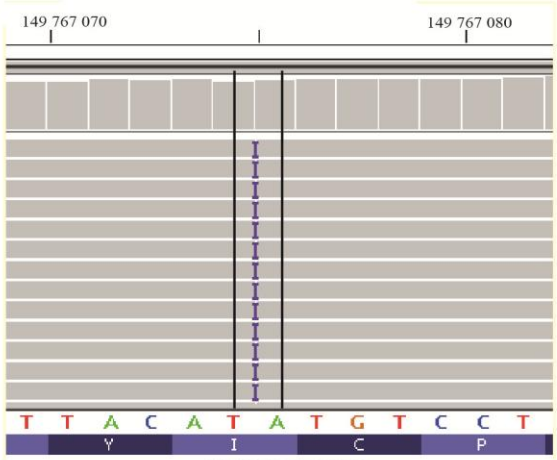

MTM1 (NM_000252.2)

c *SETX*: c.3213-3214insT, p.Gln1072SerfsX3
heterozygous insertion
patient D

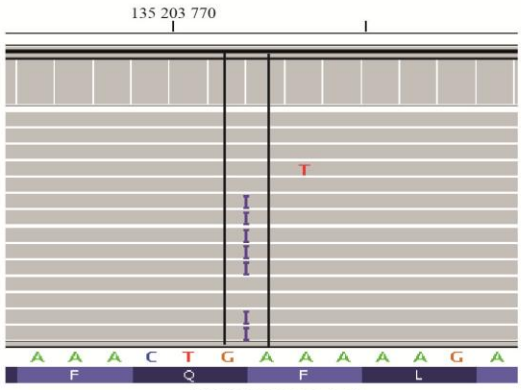

SETX (NM-015046.5)

d *SETX*: c.5275-1G>A
heterozygous intronic mutation
patient D

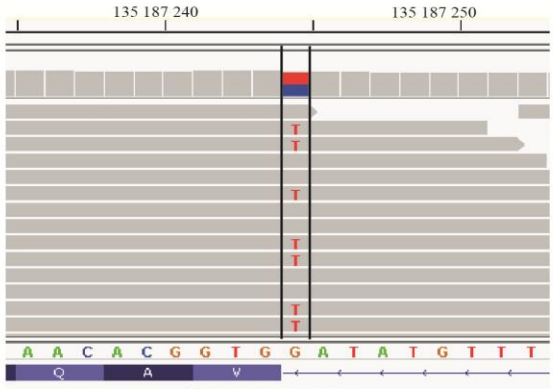

SETX (NM-015046.5)

e *DNM2*: c.1565G>A, p.Arg522His
heterozygous exonic point mutation
patient F

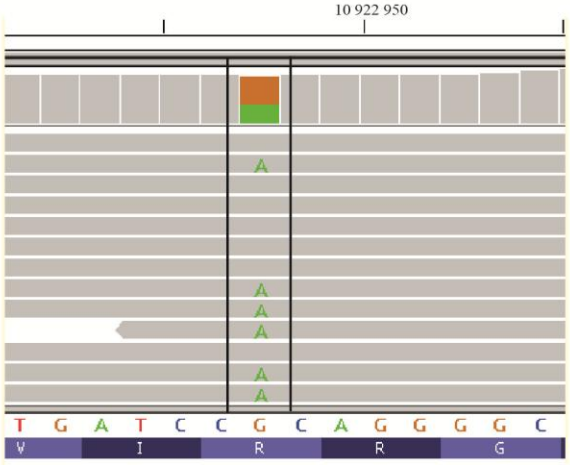

DNM2 (NM_001190716)

Online resource Fig 4: Detection of novel mutations. a) and b) Detection of compound heterozygous mutations in the *TTN* gene in a patient with limb girdle muscular dystrophy (patient O). The mutations in exons 18 and 240 are c.3100G>A, p.Val1034Met and c.49243G>A, p.Ala16415Thr. c) Detection of a heterozygous mutation in the *TTN* gene in a patient with myopathy with cytoplasmic aggregates (patient J). The mutations in exon 292 is c.68576C>T, p.Pro22859Leu. d) Detection of an exonic heterozygous point mutation in the *COL6A3* gene in a patient with autosomal dominant Bethlem/Ullrich syndrome (patient K). The mutation in exon 27 is c.6812G>A, p.Arg2271Lys. e) Detection of monoallelic heterozygous variations in the *LMNA* gene in a patient with axonal neuropathy (patient N). The variations in exon 11 are c.1928C>A, p.Thr643Asn and c.1930C>T, p.Arg644Cys. The p.Arg644Cys change was previously reported as pathogenic in laminopathies. Figures displayed with the integrative genomics viewer IGV. The normal nucleotide and protein sequences are depicted at the bottom.

a *TTN*: c.3100G>A, p.Val1034Met
heterozygous point mutation
patient O

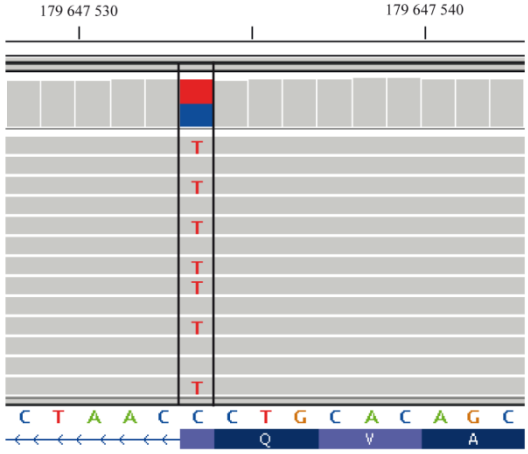

TTN (NM_133378.4)

b *TTN*: c.49243G>A, p.Ala16415Thr
heterozygous point mutation
patient O

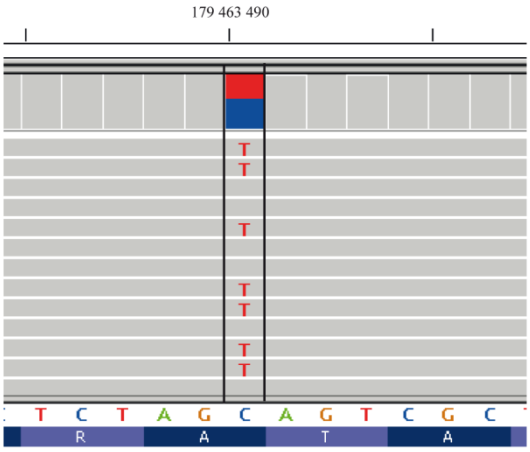

TTN (NM_133378.4)

c *TTN*: c.87491C>T, p.Pro29164Leu
heterozygous point mutation
patient J

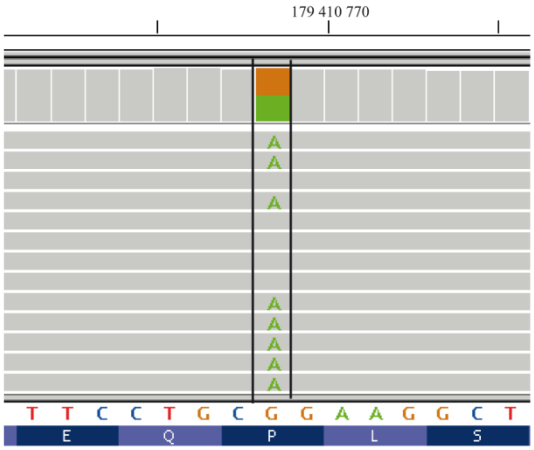

TTN (NM_133378.4)

d *COL6A3*: c.6812G>A, p.Arg2271Lys
heterozygous point mutation
patient K

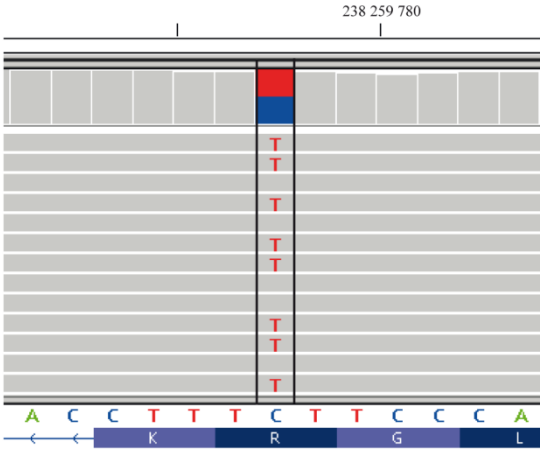

COL6A3 (NM_004369.3)

e *LMNA*: c.1928C>A, p.Thr643Asn; c.1930C>T, p.Arg644Cys
monoallelic heterozygous
patient N

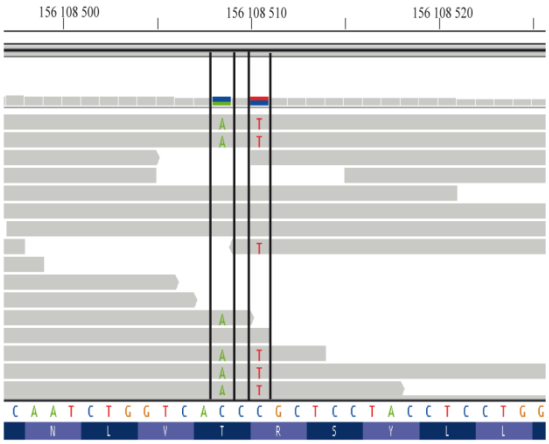

LMNA (NM_170707.2)

Online resource Table 1: List of the 267 targeted neuromuscular disease genes and associated diseases.

Online resource Table 2: Coordinates, GC content and mean coverage of targeted exons in each patient.

Online resource Table 3: Variants ranking, conservation scores and amino acid change scores.

Online resource Table 4: Sequencing, coverage and variant statistics for patients with previously unknown mutations.

References

1. Edstrom, L., Thornell, L.E., Albo, J., Landin, S., and Samuelsson, M. (1990) Myopathy with respiratory failure and typical myofibrillar lesions. *J Neurol Sci* 96, 211-228
2. Lange, S., Xiang, F., Yakovenko, A., *et al.* (2005) The kinase domain of titin controls muscle gene expression and protein turnover. *Science* 308, 1599-1603

Supplementary Table 3: Variants ranking, conservation scores and amino acid change scores

Patient	Type of mutation	Gene	Mutation nucleotide (protein)	Sequence reads	Prediction with SIFT or polyphen	VaRank ranking for all 267 NMD genes	VaRank ranking for disease class [4]
A	Indel	*MTM1*	c.141-144delAAAG (p.Glu48LeufsX24)	125 / 87	n.a.	2	1
B	Exonic point mutation	*BIN1*	c.1717C>T (p.Gln573X)	0 / 11	n.a.	3	1
C	Large deletion	*DMD*	Deletion ex18-44	n.a.	n.a.	large deletion found	large deletion found
D	Indel + intronic splice site mutation	*SETX*	c.3213-3214insT (p.Gln1072SerfsX3); c.5275-1 G>A	129 / 102; 66 / 67	n.a. - n.a.	2 [2]	1 [2]
E	Indel	*MTM1*	c.156-157ins A (p.Cys53MetfsX8)	6 / 96 [3]	n.a.	2	1
F	Exonic point mutation	*DNM2*	c.1565 G>A (p.Arg522His)	25 / 17	Probably damaging	7	1
G	Intronic, effect on splice	*MTM1*	c.1261-10A>G	0 / 80	n.a.	28	1
H	Indel + exonic point mutation	*SETX*	c.2967-2971delGAAAG (p.Arg989SerfsX5); c.994 C>T (p.Arg332Trp)	57 / 116; 74 / 161	n.a. - Deleterious	2	1 [2]
I	not found	none			n.a.		
J	Exonic point mutation	*TTN*	c.68576C>T (p.Pro22859Leu)	137/131	Deleterious	3	1
K	Exonic point mutation	*COL6A3*	c.6812G>A (p.Arg2271Lys)	37 / 36	Possibly damaging	28	3 [5]
L	not found	none			n.a.		
M	not found	none			n.a.		
N	Exonic point mutation	none (LMNA)	c.1928C>A (p.Thr643Asn); c.1930C>T (p.Arg644Cys 2)	13 / 11; 13 / 11	Deleterious - Deleterious	13	1 [2]
O	Exonic point mutation	*TTN*	c.3100G>A (p.Val1034Met); c.49243G>A (p.Ala16415Thr)	162 / 131; 72 / 75	Deleterious - Deleterious	7	1 [2]
P	Exonic point mutation	*RYR1*	c.8554C>T (p.Arg2852X); c.11557G>A (p.Glu3853Lys)	69 / 45; 23 / 34	n.a. - Deleterious	2 [2]	1 [2]

[1] reads for WT/mutant allele

[2] in a recessive scenario

[3] 94% reads show the variant and the heterozygous limit was set to 80%